

## Developing Ball Pulse Generator in Piezoelectric Transduction Designed on Wireless Sensing Devices

Gulhabib Hanifi<sup>1</sup> and Tooryalai Hamdard<sup>2</sup>

<sup>1</sup>Lecturer of Physics Department, Education Faculty, Ghazni University, Ghazni AFGHANISTAN.

<sup>2</sup>Lecturer of Basic Science Department, Medical Faculty, Nangarhar University, Nangarhar AFGHANISTAN.

<sup>1</sup>Corresponding Author: [gulhabib.091@gmail.com](mailto:gulhabib.091@gmail.com)



[www.ijrah.com](http://www.ijrah.com) || Vol. 2 No. 6 (2022): November Issue

Date of Submission: 20-11-2022

Date of Acceptance: 24-11-2022

Date of Publication: 28-11-2022

### ABSTRACT

Progressing Ball pulse generator through piezoelectric transduction is designated in this paper directed on wireless recognizing procedures. A silver rolling ball is stimulated popular the original through method of an inertial proof mass motivated finished outside waves at random low frequency. Winning development of the metallic resistant mass, magnetic construction can be extended near motivate the piezoelectric cantilever finished awarding tip magnets near the acceptable completion. Prevalent accretion, self-synchronous switching is achieved via relating electrodes toward the path of the developing ball. An unique passive prebiasing instrument is familiar toward advance the presentation of the pulse producer. Together simulation also new results continued showed near determine the expansion. Experimental results rally supplementary energy container remains impassive through the prebias instrument associated near the impartial occasion. A announcement circuit founded decided a Colpitts oscillator stayed constructed toward examination the presentation of the capacitor-powered oscillator which remains calculated in way of the load of the pulse generator. Through addition a voltage regulator element, the transmission circuit is accomplished of software design an instrument signal via frequency intonation which controls the possibility of affecting a developing ball wireless sensing original founded decided the piezoelectric pulse generator.

**Keywords-** Energy harvesting, piezoelectric energy, Piezoelectric Transduction, Piezoelectric pulse generator, wireless recognizing.

### I. INTRODUCTION

BY a growing demand arranged reduced electronic devices aimed at body sensor networks then wearable wireless sensing techniques, the conservation issue of batteries has become a major drawback. Aimed at Internet of Effects applications in specific wherever electronic functionality is further toward actual great numbers of autonomous items maintenance-free influence facility is a critical enabler. Exploring sustainable influence bases consumes converted a prevalent issue directing toward spread the life- time then meet the obligation of contracted devices<sup>[1]</sup>. Numerous methods with exploitation of bright besides temperature differences must remained applied by way of influence provisions<sup>[2]</sup>,<sup>[3]</sup>. Ambient wave stays extra

hopeful energy foundation that has drawn growing examination attention then inertial energy harvesters need showed toward is an outstanding candidate by way of a control basis<sup>[4]</sup>. A self-powered wireless sensor network (WSN) node plat- arrangement takes been described through our collection by electrostatic transduction<sup>[5]</sup>. A metallic rolling stick remained included into the original by way of an outside impervious mass, such that it could be excited through random low incidence. This pattern changes energy after ambient indications toward electrical energy then increases it through movable capacitances aimed at wireless transmission. This policy determines a different thought aimed at immediate wireless sensing by energy harvesting techniques. Though due toward the short variable capacitances achievable since electrostatic

trans- diction the energy extracted after the device is identical imperfect then only 2 NJ per operational rotation can be harvested. Piezoelectric transduction takes involved significant investigation interest besides has been showed by way of an outstanding technique in terms of energy generation [6], [8]. Through the rolling stick by way of an outside resistant mass, a piezoelectric energy harvester has been considered [9]; the original demonstrations decent performance aimed at energy harvesting but cannot be practical toward wireless sensing straight. Via relating the structures of the double devices in [5] and [9], a rolling ball pulse generator through piezoelectric transduction has been established then is obtainable here. This device delivers substantial output, which can be applied straight by way of a power foundation aimed at its load circuit therefore that a rolling ball wireless sensing sample can be designed created on this device. The piezoelectric pulse generator involves of double quantities, which remain:1) the electromechanical prototype besides 2) the middle circuit. The electromechanical quantity is motivated through ambient wave besides generates energy through piezoelectric transduction. The circuit amount is planned toward store a fixed amount of energy then discharges it into the following stage load circuit in all operating rotation. This paper offerings the construction and the operational principle of the pulse generator. Consequences together since simulations and experiments are providing toward demonstrate the performance of the device. A passive prebias mechanism is familiarized toward increase the amount of energy removed in all operating cycle, and is too established together since simulations and experiments. A capacitor-powered oscillator is considered and tested as the load of the pulse generator and a frequency modulation method is added aimed at wireless sensing.

## II. ENERGY COLLECTION BY APPROACH OF PIEZOELECTRIC TRANSDUCTION

The building of the rolling ball prototype is offered in Figs. 1 and 2. By way of explained in the figures, the substrate of the method is completed of glass plates. A piezoelectric beam is due in the substrate, and double magnets  $M_1$  and  $M_2$  are involved toward the free finale of the beam aimed at suitable magnetic strength. A steel rolling ball, which is on in the V-groove track of the substrate, is used by way of an outside proof mass and Motivated through the groundswell source. In calculation the metallic rolling spheres procedures magnetic connection together through the tip magnets on the piezoelectric beam while it rolls along the track. The electrodes  $E_1$  and  $E_2$  are used as a self-synchronized switch once the prototype is related toward an electrical load.

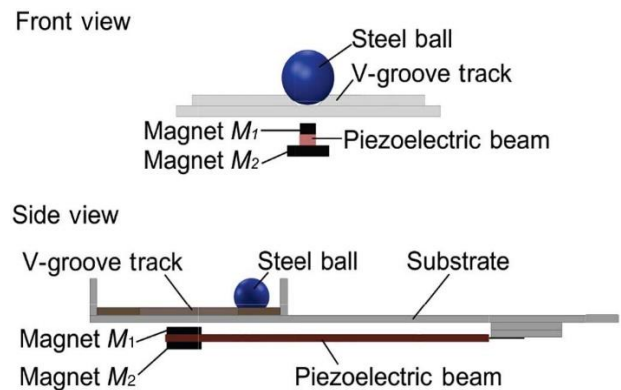


Figure 1: Building of the rolling ball prototype.

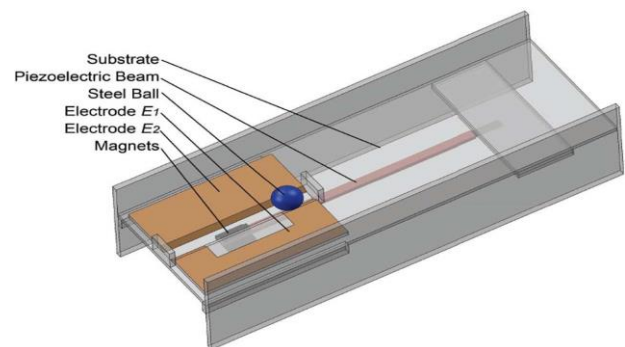
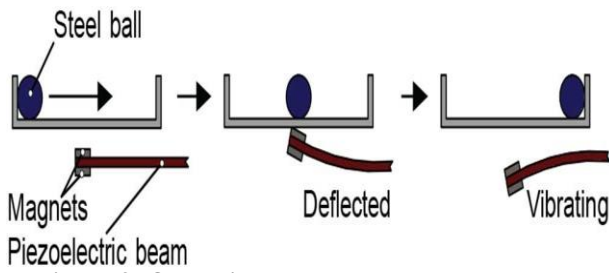
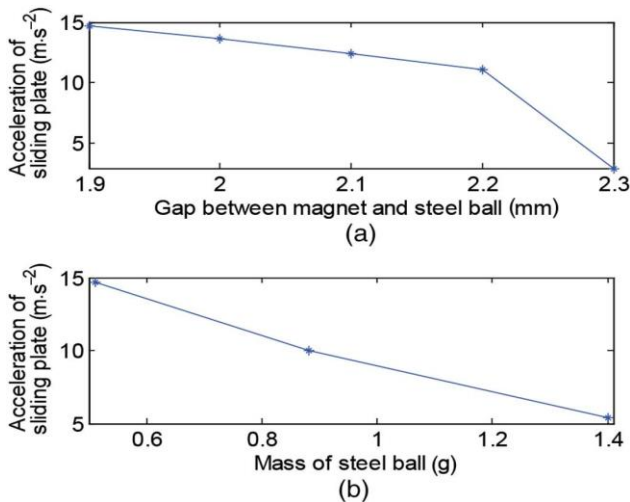


Figure 2: Element calculations of the electromechanical prototype.

Piezoelectric energy generation is conventionally considered and used in constant base excitation such as in [10]. Complete applying the outdoor rolling proof mass toward the prototype through method of presented in Fig. 2, the piezoelectric beam can be actuated dis- continuously through the magnetic coupling among the metallic rolling ball and the tip magnets. Though the device is motivated via a responding outside motion horizontally (this is delivered in a sliding plate organized through a servo drive by way of Kollmorgen, proceeding which the method is mounted in the experiments), the rolling ball can travel back and forth from any end-stop toward the additional through the V-groove track. Fig. 3 shows the operating process of the device in every cycle. Through way of shown in the figure, when the ball reaches the middle of the track, the magnetic power between the ball and the tip magnets deflects the piezoelectric beam, and after the rolling ball transfers away from the tip magnets, the beam is free toward vibrate. Piezoelectric energy can be generated both from the deflection and the vibration, and this progression pronounced above is defined by way of one effective series of this device. In order toward achieve the function described above, the magnetic join must be high enough to deflect the piezoelectric beam, and the acceleration of the external motion must be sufficient toward release the ball after the magnet. Fig. 4 explains the smallest acceleration required aimed at the external indication in different situations.



**Figure 3: Operative process through the steel ball actions from one end-stop toward other.**

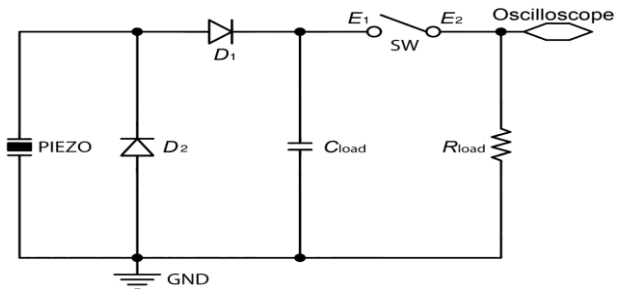


**Figure 4: Dynamic analysis excited through the slider: smallest outside acceleration required toward release. the steel ball from the magnets.**

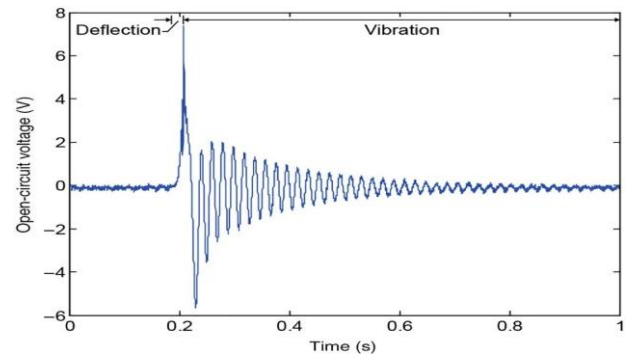
In Fig. 4(a), a 5-mm diameter steel ball (0.5 g) is used, and the opening among the magnet and the steel ball is definite by way of the distance between the bottom of the ball and the top surface of magnet  $M_1$  in Fig. 2 when the beam is deflected. By way of can be seen from the figure, through growing the gap the outside acceleration necessary is decreased. But, the tradeoff is that the decrease of the gap results in a reduced beam deflection, which decreases the energy generated from the beam. In Fig. 4(b), balls by dissimilar weights are used toward analyze the impression of the motion on the prototype when the gap is permanent at 1.9 mm, and the Smallest acceleration required aimed at external motion is reduced with increasing proof mass, which indicates that the ball with larger weight can more easily escape the magnetic power.

Fig. 5 demonstrates the experimental result from the electromechanical prototype, and the open-circuit voltage in unique operating cycle is plotted in this figure. By way of can be seen from the plot, primarily a affirmative pulse is generated when the beam is refracted. The rest of the resonant waveform is from the vibration of the ray. This production result determines a beneficial energy harvesting performance dissimilar toward the stick proof mass device [9]. Though, this electromechanical prototype is not straight appropriate by way of a power supply aimed at signal sensing and

wireless transmission, subsequently the production voltage is not rectified. Through applying an intermediate circuit toward the prototype, the output energy can be transformed into relatively unceasing influence, which is extra compatible with wireless signal processing.



**Figure 5: Open circuit measurement.**



**Figure 6. Diagram of the intermediate circuit.**

### III. EVALUATION BETWEEN UNBIASED AND PRE-BIASED SES

The mathematical analysis is also applied to this prototype using the same method in last section and the simulation results are plotted in Figure 7. And .8. In the unbiased case, the load capacitor extracts energy during the initial deflection of the beam and the first two positive vibrations, and the final amplitude of the voltage on  $C_{load}$  is 5.3 V. The pre-biased case shows that most of the charge is extracted from the first positive peak to  $C_{load}$ , when the beam starts to vibrate, and according to the analytical result, the voltage on  $C_{load}$  is 7.2 V.

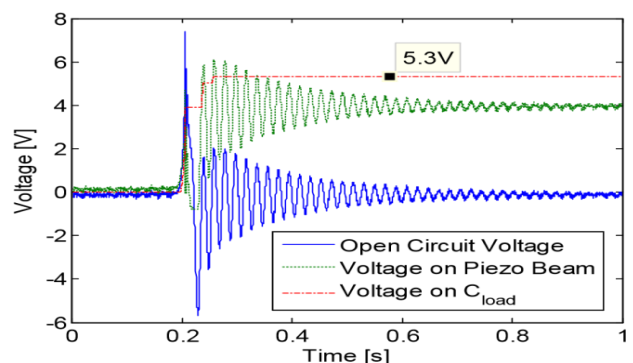


**Figure 7: Analytical result: unbiased case.**

By comparing the simulated results among the unbiased and pre-biased cases, the output voltage is increased through 36%, which further demonstrates the pre-biased case can dramatically improve the performance of the pulse generator.

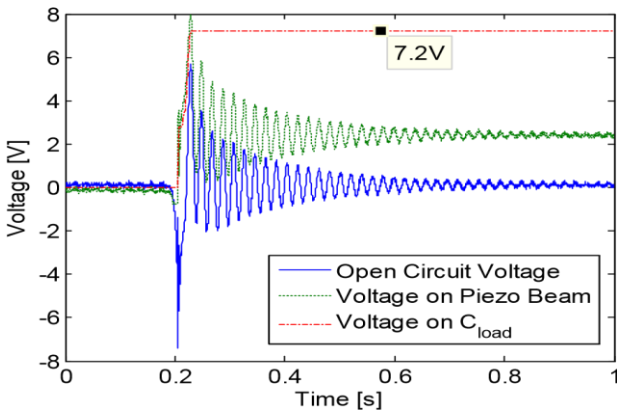


Figure 8: Analytical result: pre-biased case.

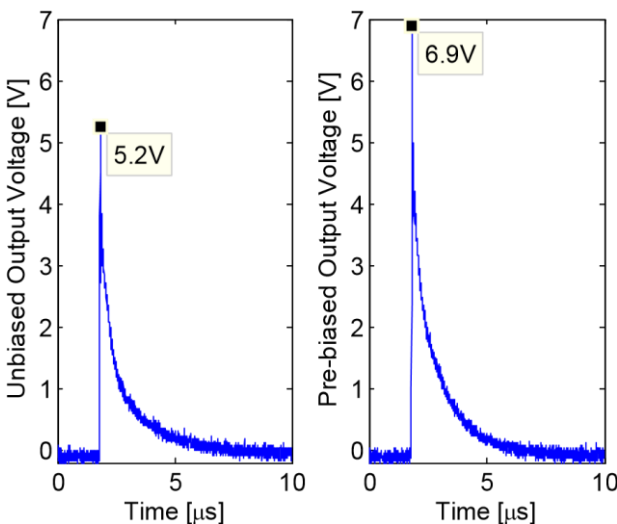


Figure 9: Production voltages measured in the unbiased and pre-biased cases.

Figure 9. Illustrations the output voltages through a load resistor of 50 Ω in the unbiased and pre-biased cases respectively. As shown in the plots, the load capacitor manages to extract the piezoelectric energy and store it for the next stage load circuit. The plots toward demonstrate that the ball-electrodes switch can be used as self-synchronous switching for connection and disconnection between the pulse generator and the load when the device is operating. In addition, the output voltages are regulated to pulses via the intermediate circuit instead of resonant waveforms in Figure 9.

By way of presented in Figure 9., the amplitude of the pulse is 5.2 V in the unbiased case and 6.9 V in the pre-biased case, and the voltage is increased by 33%, which also indicates the validity of the simulation result.

According toward the measurements, the unbiased energy exacted per cycle is 135 NJ, and the

pre-biased energy per cycle is 238 NJ. This demonstrates that by using the pre-biasing method in this rolling ball prototype, the energy extracted per pulse is increased via 76%. This pulse generator can achieve its function as well as the large-scale one by combining physical contacts as a mechanical switch and diodes as an electric switch. But it is worth pointing out that the physical contacts made by the steel ball and the copper tapes may inject noise to the output of the pulse generator due to the dynamic contact resistance when the ball is travelling. In addition, the deformation of the piezoelectric beam may result in slight change of the piezoelectric capacitance, which may also influence the charge sharing process between the load capacitor and the piezoelectric capacitor.

### 3.1 Analytical Model expected through the Unbiased and Prebiased Pulse Generator

Dissimilar demonstrating methods have been used toward evaluate the performance of piezoelectric generators such by way of [13] and [14]. In instruction toward analyze the progression of the offered piezoelectric pulse generation in detail and examine the passive prebiased method toward progress the presentation a piezoelectric simulation model constructed arranged the recent prototype was designed toward simulate the charge sharing process while the pulse generator is operating.

The objective of the simulation model is toward use the open-circuit voltage measured from the electromechanical prototype immediate analyzing the quasi-static electrical performance of the piezoelectric beam and the load capacitor during operation. Fig. 8 demonstrates the construction of the model. By way of presented in the block illustration the open-circuit voltage from the electromechanical part is the input data toward the model, and the outputs are the voltages arranged the piezoelectric cantilever and the load capacitor. This model can be recognized by way of the linear relationship between the displacement of the piezoelectric beam and the surface charge preceding it, when it operates in open circuit [15].

In order toward simplify the analysis of the quasi-static performance of the piezoelectric beam, a few assumptions are made, which are: 1) the mechanical behavior of the piezoelectric beam is not influenced through the surface charge loss; 2) the piezoelectric beam has no leakage; 3) the capacitance of the load capacitor is equal toward the piezoelectric capacitance; and 4) the diodes are assumed as having a finite threshold voltage  $V_{th}$  but otherwise ideal. Under the conventions, the piezoelectric beam has three promising situations when the circuit in Fig. 6 is connected toward it.

If the piezoelectric beam makes  $D_2$  accelerative biased, the surface voltage is

$$V_{piezo}(t) = -V_{th} \tag{3}$$

Where  $V_{th}$  is the beginning voltage of the diode.

Throughout the process the load capacitor stays in double surroundings. When  $D_1$  is forward biased the load capacitor extracts charge from the piezoelectric beam, accordingly the voltage on the load capacitor at time  $t$  can be simulated by way of

$$V_{load}(t) = V_{piezo}(t) - V_{th} \quad (4)$$

Wherever  $V_{load}$  is the voltage on  $C_{load}$ . When  $D_1$  is opposite biased, the voltage stays constant, so the Voltage on  $C_{load}$  is  $V_{load}(t) = V_{load}(t - \Delta t)$ .

The piezoelectric model described overhead remained coded in MATLAB and Fig. 10 presents the simulation results. The data of the open-circuit voltage was measured from the prototype, which is the same as the one shown in Fig 5. According toward the plots, the load capacitor extracts energy during the preliminary deflection of the beam and the first two affirmative vibrations, and the ultimate amplitude of the voltage on  $C_{load}$  is 5.3 V.

Through the identical analytical model, the prebiased case can be estimated through.

Reversing the polarity of the beam. In this case the input data is  $1 V_O(t)$ , where  $V_O(t)$  is the measured open- circuit voltage used in the unbiased case; the results are publicized in Fig. 12. Best of the charge is extracted from the first affirmative peak toward  $C_{load}$ , when the beam starts to vibrate, and according toward the simulation result, the voltage on  $C_{load}$  is 7.2 V.

Through comparing the simulated results among the unbiased and prebiased cases, the output voltage is increased by 36%, which demonstrates that the prebiased case can dramatically increase the performance of the pulse generator.

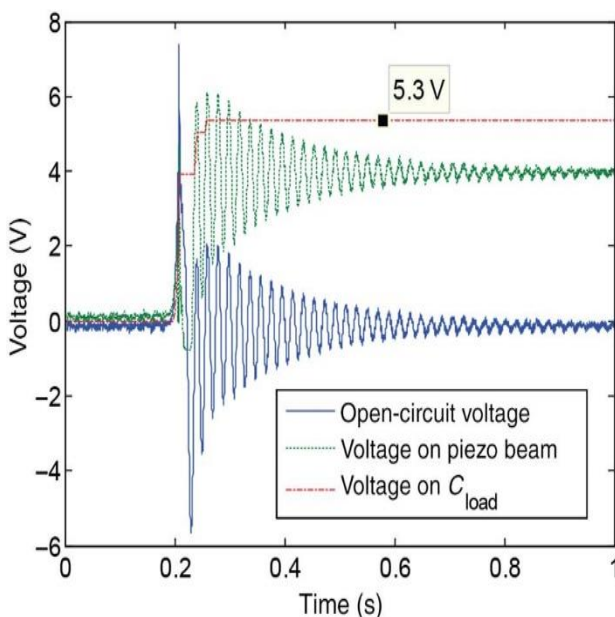


Figure 10: Simulation of the piezoelectric model.

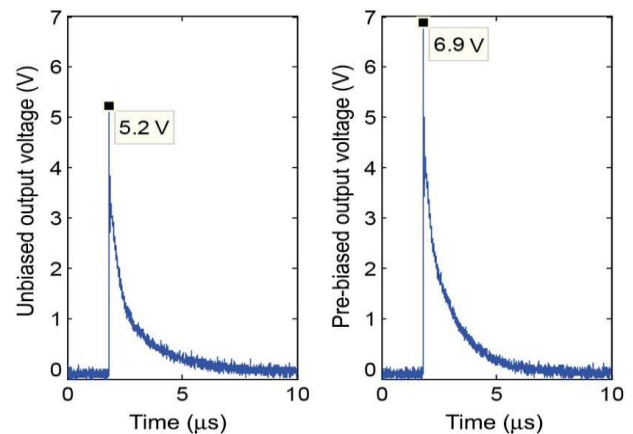


Figure 11: Simulation result of the pulse generation.

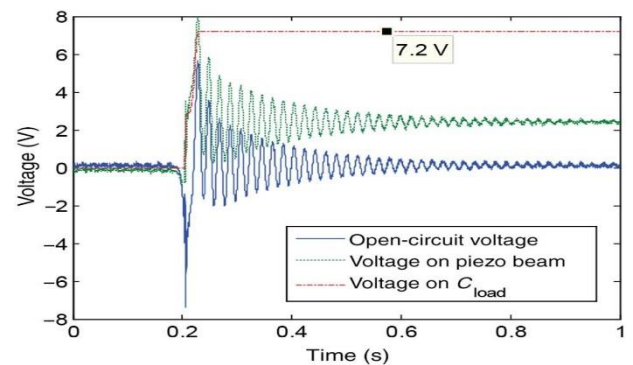


Figure 12: Experimental results: output pulses generated with and without prebiased piezoelectric beam.

Measurement of the cantilever is 38 mm, which is the main factor toward restrict the dimension of the device (75 mm × 27 mm × 25 mm). Binary magnets (N45 neodymium) are chosen by way of the tip magnet aimed at magnetic connection and the dimensions are 5 mm 1.5 mm 1 mm aimed at  $M_1$  and 5 mm 4 mm 1.5 mm for  $M_2$  as shown in Fig. 2. The capacitance of the piezoelectric beam is 10 nF aimed at each of the piezoelectric layers and one layer is used in this prototype. The capacitance of the load capacitor is 10 nF toward match the piezoelectric capacitance, and the double diodes  $D_1$  and  $D_2$  are both BAS45A low-leakage diodes. The electrodes  $E_1$  and  $E_2$  are made of copper tapes and attached concluded the V-groove track. The proof mass of the pattern is a 5 mm diameter steel ball, whose mass is 0.5 g. In the experiment, a resistor of 50  $\Omega$  is used as the load of the device. Fig. 13 demonstrates the output voltages measured across the load resistor in the unbiased and prebiased cases, individually. By way of shown in the plots, the load capacitor manages toward abstract the piezoelectric energy and store it aimed at the next stage load circuit. The plots also demonstrate that the ball-electrodes switch can be used by way of self-synchronous switching for connection and dis-connection between the pulse generator and the load when the device is operating. In addition, the output voltages are regulated

toward pulses through the intermediate circuit instead of resonant waveforms in Fig. 5.

Through way of presented in Fig. 11, the amplitude of the pulse is 5.2 V in the unbiased case and 6.9 V in the prebiased case, and the voltage is improved through 33%, which specifies the validity of the simulation result. As the piezoelectric charges are stored in the load Capacitor in both operative cycles, the energy per cycle can be estimated by way of load.

$$E=C$$

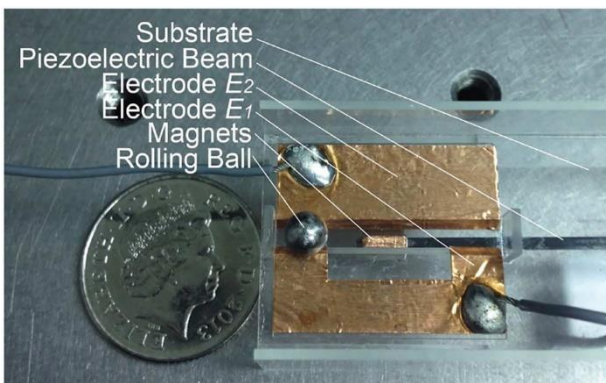


Figure 13: Experimental model of the piezoelectric pulse generator.

### 3.2. Investigational Structure and Measurements

As offered in Figure 14, a large-scale model was set up to verify the proposed concept of the piezoelectric pulse generator. Electrodes  $E_1$  and  $E_2$  are made of copper tape, and are attached through the track of the rolling rod. The beam, which is a piezoelectric bimorph from Johnson Matthey, is fixed by a clamp on the substrate. The free length of the bimorph is 38 mm. The capacitance for each piezoelectric layer is  $\sim 45$  nF, and only one layer is used in this prototype. A square window is made on the substrate, which allows the laser sensor to be mounted under the generator for measurement. In order to actuate the piezoelectric beam, a block magnet (N45 neodymium) is used with dimensions 5 mm  $\times$  4 mm  $\times$  1.5 mm. The mass of the metal rolling rod is 390 g.

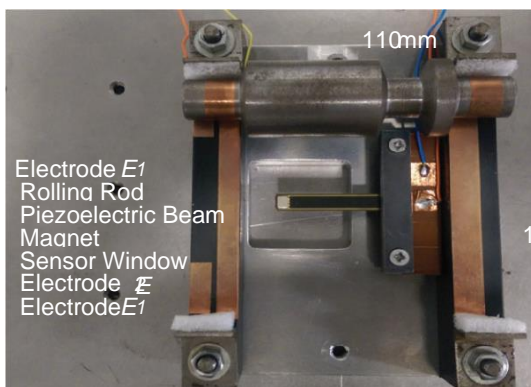


Figure 14: Rolling rod generator of the experimental set-up.

Exposed circuit measurement is made through using the set-up without the load circuit described in Figure 6, and a laser displacement sensor (Keyence LK-H052) is used to measure the tip displacement of the beam. The results are shown in Figure 14. As can be observed from the voltage plot, the first two positive peaks are generated when the piezoelectric beam is deflected. As illustrated in Figure 15, the tip displacement is not constant during one pass of the rolling rod, and as the amplitude of the open circuit voltage is proportional to the tip displacement of the beam, the first pulse occurs instantaneously when the magnet touches the rod and the second pulse occurs just before the beam is free to vibrate. In addition, the amplitude of the second pulse is larger than the first one. This is because the rod pulls the tip of the beam to a higher position before it frees the beam, making  $h_3$  larger than  $h_1$  in Figure 16. Apart from the deflection pulses, the rest of the resonant waveform in Figure 15 is from the vibration after the rod moves away from the beam.

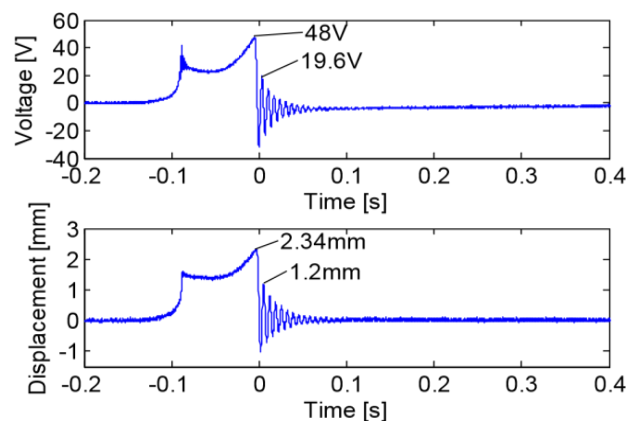
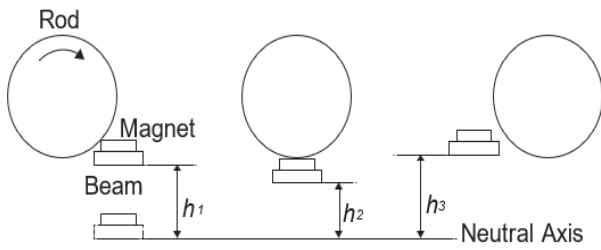


Figure 15: Measurement result of the open circuit voltage and tip displacement of the piezoelectric beam.

It is value pointing out that the maximum voltage amplitude during the deflection is much higher than the first positive vibration peak as shown in Figure 14, which also can be observed from the tip displacement of the piezoelectric beam. This phenomenon occurs because in practice the magnetic force does not vanish instantly when the rod rolls away from the tip magnet. In addition, by comparing the two plots in Figure 15, when the tip displacement goes back to the neutral axis, the voltage of the beam does not completely vanish. This is caused by the charge leakage through the internal impedance of the probes for the measurement.

The open circuit measurement indicates brilliant performance as an energy harvester, but as the output depends on the mechanical behavior of the rod and the natural frequency of the beam, it is not directly suitable for use in WSN nodes. By connecting the circuit of Figure 16 to the piezoelectric-beam



**Figure 16: Successful tip displacements of the piezoelectric beam.**

The energy extracted can be regulated and stored simultaneously in the load capacitor, and the stored energy can then be discharged to the external load of the pulse generator synchronously when the rod-electrode switch is closed.

The middle circuit by way of the one shown in Figure 16 is used for the experiment set-up. The diodes used in the experiment are BAS45a low leakage diodes, and the load capacitor is chosen to be 47nF to match the piezoelectric capacitor. During the measurement, the load capacitor,  $C_{load}$ , is charged and discharged once with the rod moving from one end-stop to the other and Figure 16 shows the output plot of the pulse generator in one operating cycle. As shown in the Figure, the amplitude of the pulse in each operating cycle is 39.2 V. As the energy is stored in  $C_{load}$ , the amount of extracted energy in each operating cycle is 36  $\mu$ J.

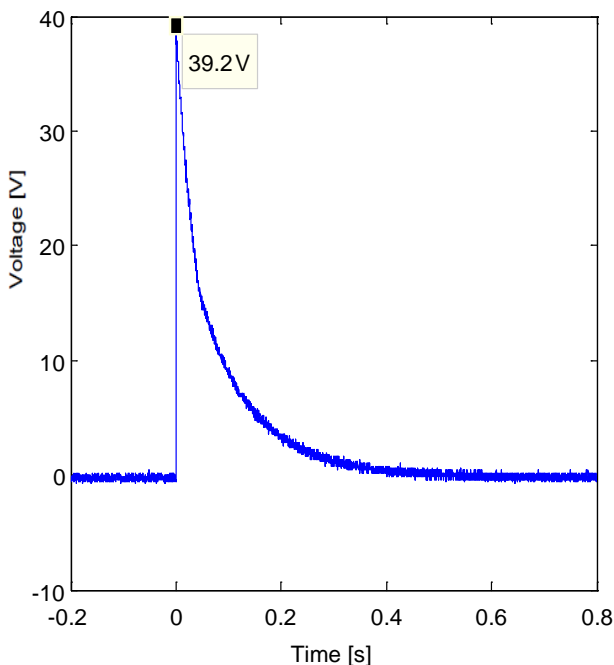


**Figure 17: Output measurement of the pulse generator with a 1 MΩ load.**

The beat generator manages to realises synchronous-switching by use of diodes as electrical switches and the rod-electrode pairs as mechanical switches. This process makes it available to generate

piezoelectric energy from ambient vibration and store it at the same time. However, according to Figure 17, the peak value of the open circuit voltage is more than 48V, whereas the amplitude of the pulse in each cycle reduces to 39.2V. This charge penalty is caused by the charge sharing mechanism between two capacitors. Since the charge sharing requires  $D_1$  to be forward biased, most of the energy is extracted and stored during the deflection and the beginning of the vibration. This means part of the energy generated from vibration is inevitably wasted. In addition, the threshold voltage of the two diodes can cause energy loss as well. Although energy up to 36  $\mu$ J can be extracted by this prototype in each operating cycle, it is still worth exploring new approaches to improve the energy extraction rate, for further miniaturization of the device.

#### IV. PULSATION STIMULATED COLPITTS OSCILLATOR

Unimportant amendment consumes been made based on the Colpitts oscillator described above so that the circuit can be pulse stimulated.

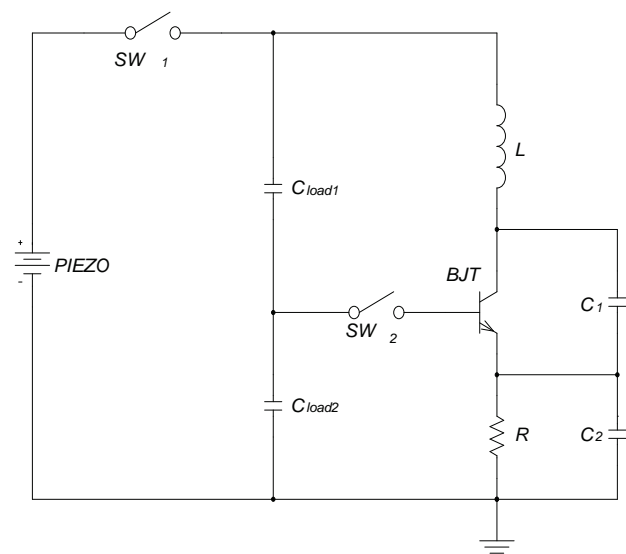


**Figure 18: Schematic of the pulse stimulated oscillator.**

Figure 18 offerings the representation of the oscillation circuit. The piezoelectric pulse generator is replaced with a DC power source  $V_{PIEZO}$  to simplify the testing. The switch,  $SW_1$ , is applied to control the connection and disconnection between the DC power source and its load. Instead of a single load capacitor in the pulse generator, this circuit requires two capacitors,  $C_{load1}$  and  $C_{load2}$ , in series, which are used not only as the impulse power supply but also to replace the two resistors in Figure 17 for bias voltage supply. Switch  $SW_2$  represents the ball-electrodes mechanical switch in the pulse generator. The right-hand side of the circuit in Figure 19 is the oscillator.

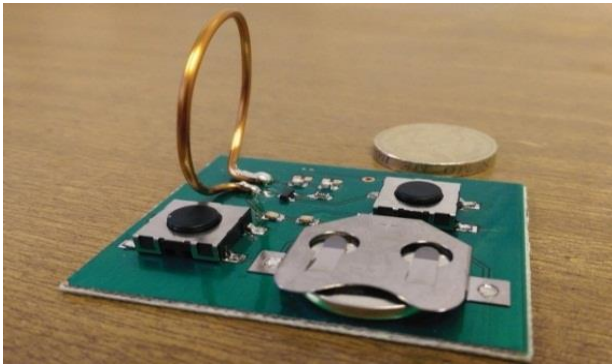


**Figure 19: Testing set-up of the Colpitts oscillator.**

The testing circuit set-up is illustrated in Figure 19. In this circuit, a loop antenna, which is made of a 1.5 mm diameter copper wire, is used, and the diameter of the antenna is 30 mm. The inductance of a loop wire can be estimated as [114]:

$$L \approx \mu_o \mu_r \frac{d_{Loop}}{2} \left[ \ln \left( \frac{8d_{Loop}}{d} \right) - \right] \quad (9)$$

Wherever  $L$  is the inductance of the loop antenna,  $\mu_o$  is the permeability of free space, which is  $4\pi \times 10^{-7}$  N/A<sup>2</sup>,  $\mu_r$  is the relative permeability of the medium, which is approximately 1 for copper,  $d_{Loop}$  is the diameter of the loop, and  $d$  is the diameter of the wire. The inductance of the loop antenna can thus be estimated as 58 nH. A coin cell battery of 3 V is used to represent the energy from the piezoelectric beam and two push button switches are used to control the circuit as shown in Figures 18 and 19. In this circuit, the mechanical switch,  $SW_2$ , is connected between the two load capacitors, which leave  $C_{load1}$  directly connected to the transmitter. This change does not cause the load capacitors to discharge before  $SW_2$  is closed, because the bipolar transistor is off without the bias voltage at the base, and in this case, the collector stops current flowing to the emitted.

The parameters of the components on the testing board are listed in Table 1.

**Table 1: Parameters of tested Colpitts oscillator**

Component	Part Number/value
VPIEZO	3 V
Cload1	22 nF
Cload2	22 nF
L	58 nH
R	1 kΩ
C <sub>1</sub>	1 pF
C <sub>2</sub>	1 pF
BJT	BFR35AP

In the examination, a loop antenna of the same size as the one for the transmitter is used to receive the transmitted signal, and is directly connected to an oscilloscope for measurement. For each of the operating cycles,  $SW_1$  is closed first to allow the two load capacitors to be charged by the battery. After the charge,  $SW_1$  turns off and  $SW_2$  is closed to provide the bias voltage to the base of the BJT. In this case, the BJT starts to operate, which is powered by the two load capacitors. After the energy stored in  $C_{load1}$  and  $C_{load2}$  cannot provide the bias voltage, the circuit stops working.

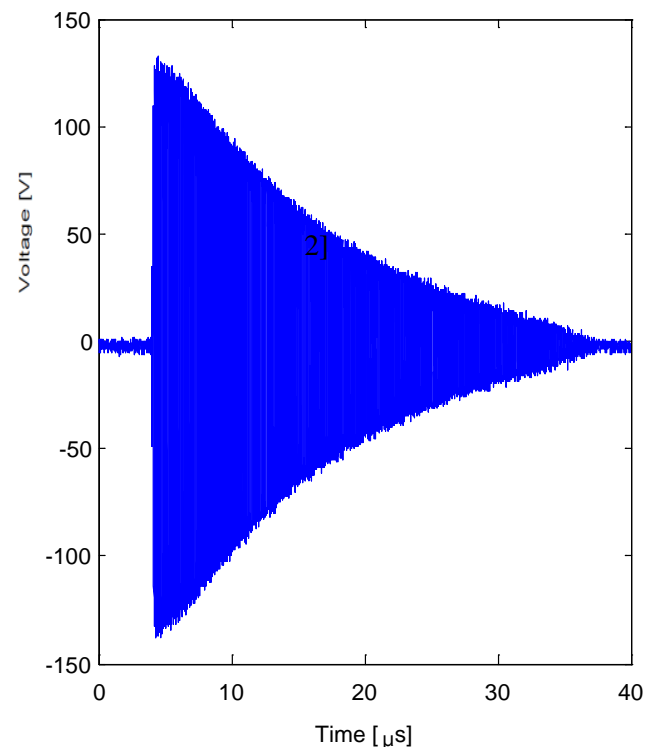


**Figure 20: Transient measurement of the received signal for one operating cycle. The transmission distance is ~ 5 cm.**

Figure 21 demonstrations the received signal in one operating cycle. The received signal shows a continuous decrease in voltage. This happens since the power is from the discharge of the two load capacitors, and the voltage across the oscillator decreases with the discharge. The time constant of the prototype is:

$$\tau = R \left( \frac{C_{load1} C_{load2}}{C_{load1} + C_{load2}} \right) \quad (10)$$

Where  $R$  is 1 kΩ, and  $C_{load1}$  and  $C_{load2}$  are both 22 nF according to Table 2. Therefore, the theoretical time constant of the circuit is 11 μs, whereas the measured time constant is approximately 13 μs in Figure 22 using curve fitting, which is very close.

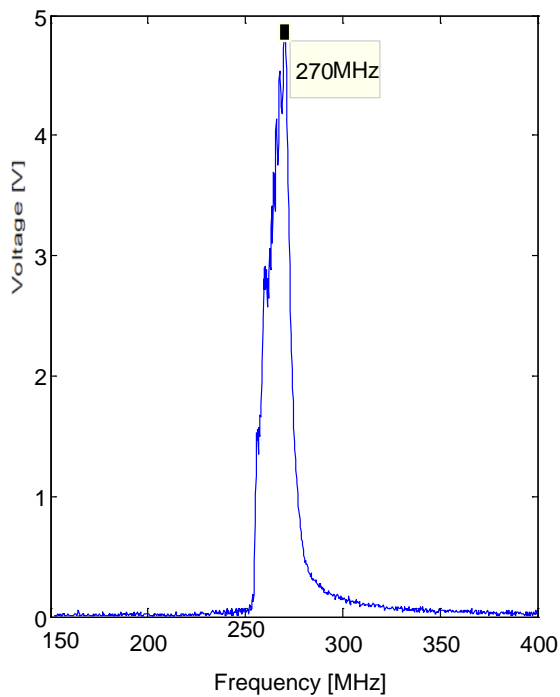


**Figure 21: Frequency analysis of the transmitted signal.**

A frequency analysis of the communicated signal is presented in Figure 21. Due to the continuous discharge of the load capacitors, the voltage across the bipolar transistor decreases. In this case, the capacitance of the transistor is changed and so does the resonant frequency of the oscillator, which causes the frequency of the signal shift from 270 MHz to 250 MHz the plot shows an asymmetric frequency spectrum, and the received amplitude decays with the decrease of frequency, which is because with lower voltage applied to the oscillator, the resonant frequency of the circuit decreases accordingly.

The experimental result establishes that the oscillator can be discretely powered by the energy stored in capacitors. However, the drawback of the design is the changes of the signal amplitude and frequency. In order to detect a signal from a sensor, such as the pH sensor in [106], a sensor input must be installed to the circuit. As has been discussed, the AM based transmission is susceptible to the noise from the environment, which makes it difficult for the receiver to filter out the signal, and requires references to calibrate the signal during demodulation. There are many other modulation techniques for wireless sensing, such as phase-shift keying, frequency shift keying and quadrature amplitude modulation<sup>[107]</sup>, but these digital modulation techniques require more complicated architecture, which is not suitable for the case that only one impulse power is provided. Therefore, with the given pulse generator as the only power source, an approach using frequency modulation is considered most suitable.

**4.1. FM Grounded Colpitts Oscillator**

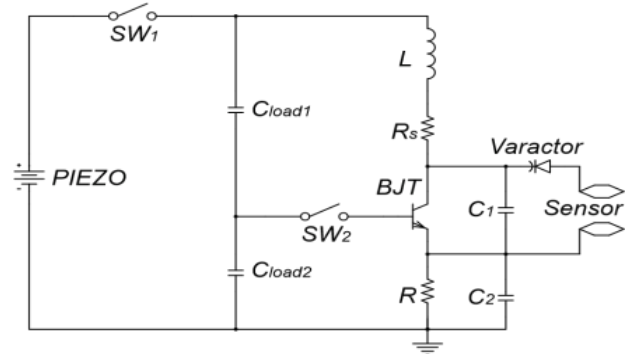


**Figure 22: Transmitter aimed at the piezoelectric generator schematic of the FM.**

In direction toward implement a frequency modulation approach to the transmitter, a reactor is connected among the transmitter and the output of the sensor to form a voltage-controlled oscillator as shown in Figure 22. Respectively time after the load capacitors are charged and SW<sub>2</sub> is closed, a signal is transmitted, with frequency range decided by the LC tank and the voltage from the sensor. In the simulation, the discharge time of the load capacitors is set at 10 μs for a clearer demonstration. It is necessary to point out that setting the discharge time is not required for the real transmitter, because different frequency ranges can be detected even if there is overlapping between them.

In this design, the smallest step of the sensor voltage is set at 0.1 V. Since the entire discharge time is very short according to Figure 22, the output of the sensor can be assumed constant in each operating cycle. This assumption defines the operating principle of the FM transmitter: in each operating cycle, the device transmitted the instant signal to the receiver, and if the frequency ranges of the received signal changes in one cycle, it indicates the sensing condition changes, and can be detected by the receiver. Table 2 gives the parameters of the FM transmitter design and Figure 22 is the transient analysis of the FM transmitter.

**Table 2: Parameters of the FM transmitter circuit.**

Component	Part Number/value
VPIEZO	6 V
Cload1	30 nF
Cload2	15 nF
L	100 nH
Rs	1.36 Ω
BJT	MMBR931
R	10 kΩ
C1	1 pF
C2	12 pF
Reactor	BBY52-02w

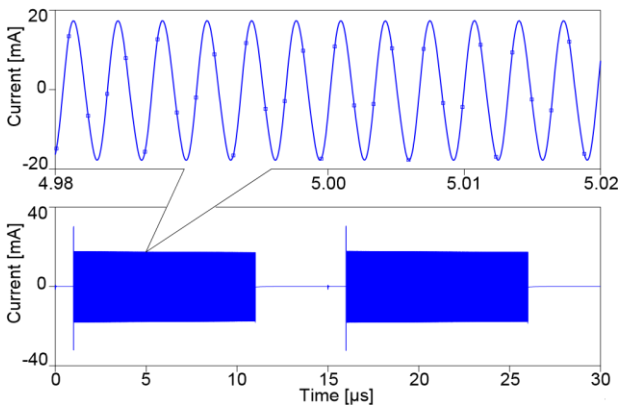


**Figure 23: Transient analysis of the FM transmitter by OrCAD (V\_Sensor =0.1 V).**

When the switch,  $SW_2$ , is closed, the LC tank oscillates at the frequency absolute by the sensor voltage for 10  $\mu s$  in each operating cycle. The frequency analysis of the current through the antenna,  $L$ , is illustrated in Figure 26 with sensor voltage trim Mable from  $-0.2 V$  to  $0.2 V$ .

As can be seen from the analysis result, the operating frequency of the FM transmitter varies between 306 MHz and 312 MHz the result provides good linearity between the operating frequency and the sensor voltage. This proves that the operating frequency of the FM transmitter can be linearly controlled by the change of the sensor voltage, and the signal from the sensor canister be modulated in the frequency domain by the transmitter.

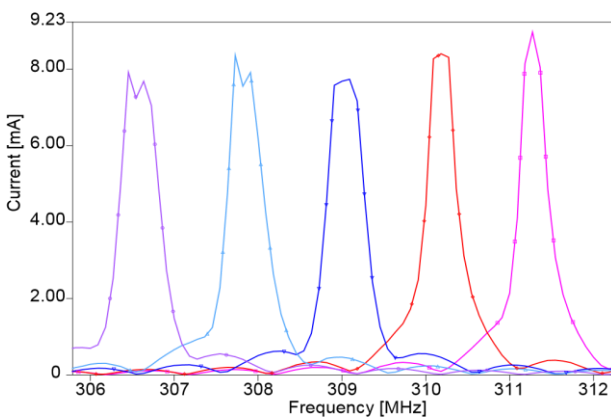


**Figure 24: Frequency analysis of the transmitter by OrCAD: with V\_Sensor increases from  $-0.2 V$  to  $0.2 V$  ( $0.1 V$  steps), the resonant frequency decreases.**

## V. CONCLUSION

A rolling ball pulse generator has been presented in this paper using piezoelectric transduction for wireless sensing. Both simulation and experiment results are illustrated to demonstrate and the simulation results demonstrate that the signal after a sensor can be encoded moreover with amplitude modulation or frequency

modulation when different load circuits are used. The experimental result from the impulse Colpitts oscillator expressions promising performance by way of the energy from the load capacitors can be successfully transmitted to the receiver. The operating principle and feasibility of this device. A passive prebias mechanism is introduced to enhance the performance of the piezoelectric pulse generator, and it was demonstrated both by simulation and experiment that the prebias method can extract 76% more energy from the device compared to the unbiased case. This result is expected to enhance the energy density of low-frequency and impulse-excited piezoelectric harvesting devices. The simulation results of the piezoelectric pulse generator are consistent with the experimental results. However, this analytical method ignores the mutual influence between the electrical changes and the mechanical changes of the piezoelectric beam, and a simulation model is under development by exploring a more comprehensive relationship between the tip displacement of the piezoelectric beam and the voltage generated.

An oscillation circuit based on a Colpitts oscillator was built to test the design when the oscillator is powered by discontinuous energy from load capacitors. The result shows promising performance as the energy from the load capacitors can be successfully transmitted to the receiver. This device could be adapted to any miniature passive sensor having a voltage output in a suitable range, such as the pH sensor in [19], thermopiles, piezoelectric strain sensors, etc. The simulation results prove that the signal from a sensor can be modulated in the frequency domain by the capacitor-powered oscillator, which demonstrates the feasibility of the proof-of-concept wireless sensing prototype based on the piezoelectric pulse generator.

## REFERENCES

- [1] O. E. Semonin *et al.*, "Peak external photocurrent quantum efficiency exceeding 100% via MEG in a quantum dot solar cell," *Science*, vol. 334, no. 6062, pp. 1530–1533, 2011..
- [2] G.-Z. Yang and M. Yacoub, *Body Sensor Networks*, 2nd ed. New York, NY, USA: Springer, 2014.
- [3] Y. Li, K. Buddharaju, N. Singh, G. Lo, and S. Lee, "Chip-level thermo- electric power generators based on high-density silicon nanowire array prepared with top-down CMOS technology," *IEEE Electron Device Lett.*, vol. 32, no. 5, pp. 674–676, May 2011.
- [4] P. D. Mitcheson, E. M. Yeatman, G. K. Rao, A. S. Holmes, and T. C. Green, "Energy harvesting from human and machine motion for wireless electronic devices," *Proc. IEEE*, vol. 96, no. 9, pp. 1457–1486, Sep. 2008.
- [5] C. He, M. E. Kiziroglou, D. C. Yates, and E. M. Yeatman, "A MEMS self-powered sensor and RF transmission platform for WSN nodes," *IEEE Sensors J.*, vol. 11, no. 12, pp. 3437–3445, Dec. 2011.

- [6] K. Cook-Chennault, N. Thambi, and A. Sastry, "Powering MEMS portable devices—A review of non-regenerative and regenerative power supply systems with special emphasis on piezoelectric energy harvesting systems," *Smart Mater. Struct.*, vol. 17, no. 4, p. 043001, 2008.
- [7] E. Aktakka, R. Peterson, and K. Najafi, "Thinned-PZT on SOI process and design optimization for piezoelectric inertial energy harvesting," in *Proc. IEEE Solid-State Sens. Actuators Microsyst. Conf. (TRANSDUCERS)*, 2011, pp. 1649–1652.
- [8] Mitcheson P D, Yeatman E M, Rao G K, et al. Energy Harvesting From Human and Machine Motion for Wireless Electronic Devices[J]. Proceedings of the IEEE, 2008, 96(9): 1457-1486
- [9] P. Pillatsch, E. M. Yeatman, and A. S. Holmes, "A scalable piezoelectric impulse-excited generator for random low frequency excitation," in *Proc. 25th IEEE Int. Conf. Micro Electro Mech. Syst. (MEMS)*, 2012, pp. 1205–1208.
- [10] A. Erturk and D. J. Inman, *Piezoelectric Energy Harvesting*. Hoboken, NJ, USA: Wiley, 2011.
- [11] J. Dicken, P. D. Mitcheson, I. Stoianov, and E. M. Yeatman, "Increased power output from piezoelectric energy harvesters by pre-biasing," in *Proc. PowerMEMS*, 2009, pp. 1–4.
- [12] D. Zhu *et al.*, "A novel piezoelectric energy harvester designed for single-supply pre-biasing circuit," *J. Phys.*, vol. 476, no. 1, p. 012134, 2013.
- [13] J. Ajitsaria, S.-Y. Choe, D. Shen, and D. Kim, "Modeling and analysis of a bimorph piezoelectric cantilever beam for voltage generation," *Smart Mater. Struct.*, vol. 16, no. 2, p. 447, 2007.
- [14] N. G. Elvin and A. A. Elvin, "A general equivalent circuit model for piezoelectric generators," *J. Intell. Mater. Syst. Struct.*, vol. 20, no. 1, pp. 3–9, 2009.
- [15] B. Richter, J. Twiefel, and J. Wallaschek, "Piezoelectric equivalent circuit models," in *Energy Harvesting Technologies*. New York, NY, USA: Springer, 2009, pp. 107–128.
- [16] B. Ziaie, K. Najafi, and D. J. Anderson, "A low-power miniature transmitter using a low-loss silicon platform for biotelemetry," in *Proc. 19th Annu. Int. Conf. IEEE Eng. Med. Biol. Soc.*, vol. 5. Piscataway, NJ, USA: IEEE, 1997, pp. 2221–2224.
- [17] C. A. Balanis, *Antenna Theory: Analysis and Design*. Hoboken, NJ, USA: Wiley, 2012.